

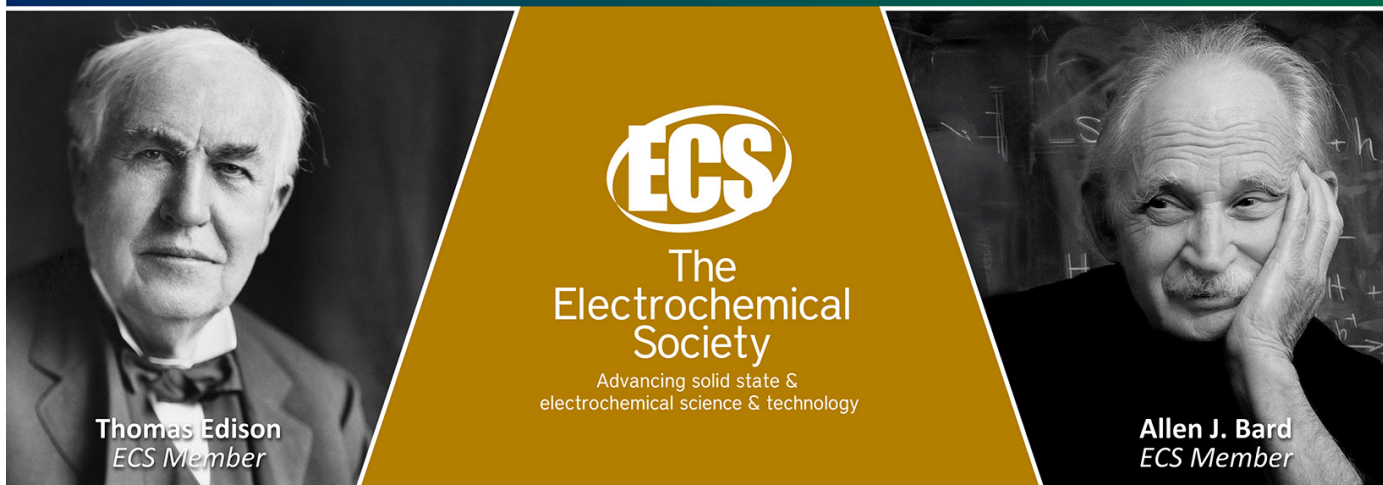
PAPER • OPEN ACCESS

The Role of Forest Fragmentation in Accelerating Soil Erosion in Mountainous Basin

To cite this article: Quang-Viet Nguyen and Viet-Huong Do Thi 2025 *IOP Conf. Ser.: Earth Environ. Sci.* **1501** 012002

View the [article online](#) for updates and enhancements.

Join the Society
Led by Scientists,
for *Scientists Like You!*



ECS
The
Electrochemical
Society
Advancing solid state &
electrochemical science & technology

Thomas Edison
ECS Member

Allen J. Bard
ECS Member

The Role of Forest Fragmentation in Accelerating Soil Erosion in Mountainous Basin

Quang-Viet Nguyen^{1*}, Viet-Huong Do Thi¹

¹ Faculty of Geography and Geology, University of Sciences, Hue University, Hue City, Vietnam

*Email: nqviet@hueuni.edu.vn

Abstract. Soil erosion is one of the most severe global threats to watershed sustainability. Fragmented forests lead to increased surface runoff, accelerating erosion, particularly in watersheds characterized by rugged terrains. Therefore, understanding the impact of forest fragmentation on soil erosion rate is crucial for effective forest and watershed management. This study applies the revised universal soil loss equation model to predict the annual average soil erosion rate and then combine it with the sediment delivery ratio to estimate sediment yield. Forest fragmentation is analyzed using a land use/land cover map derived from Landsat image, which classifies the landscape into five categories: interior, patch, transitional, edge, and perforated. The results show that the Zhoushui River Basin experiences a severe impact from soil erosion, with a mean rate of 108.47 t ha⁻¹ yr⁻¹ and a mass sediment load of 206.03 × 10⁶ t yr⁻¹ downstream, despite forests covering 76.04% of the total area. The RUSLE-SDR model shows predicted sediment yields that align closely with observed sediment discharges in the sub-basins, with a percent bias ranging from 0.75% to 24.96%. Soil erosion is particularly severe in areas affected by forest fragmentation, averaging over 100 t ha⁻¹ yr⁻¹. Among the different fragmentation classes, patches experience the highest erosion rates at 266.18 t ha⁻¹ yr⁻¹, followed by transitional areas at 225.72 t ha⁻¹ yr⁻¹. Interior areas have the lowest erosion rate at 114.10 t ha⁻¹ yr⁻¹, while edge and perforated classes experience rates of 136.63 and 188.76 t ha⁻¹ yr⁻¹, respectively. These findings would be helpful for prioritizing forest management across different forest fragmentation classes. Given the complex factors influencing on soil erosion, it is necessary to implement additional control measurements along with forest planting, particularly engineering solutions, to effectively mitigate soil erosion and sediment loads.

1. Introduction

Human-induced soil erosion causes unexpected damage to soil productivity, lifespan reservoirs, water environment, and biodiversity [1]. Watershed management needs to conserve different kinds of soil, water, and plants within a catchment to optimize their benefits to human



Content from this work may be used under the terms of the [Creative Commons Attribution 4.0 licence](https://creativecommons.org/licenses/by/4.0/). Any further distribution of this work must maintain attribution to the author(s) and the title of the work, journal citation and DOI.

beings. Land use planning and control measurements of soil erosion are crucial for effective watershed management. Spatial patterns of soil erosion intensity provide valuable information for planning soil and water conservation [2]. Soil erosion modeling is an effective tool for the stakeholders in establishing land use scenarios [3].

The revised Universal Soil Loss Equation (RUSLE) is a well-known model for estimating the annual soil erosion rate, even if it cannot account for gully erosion, channel erosion, and sediment transport [4]. The RUSLE combines with sediment delivery ratio (SDR) to estimate sediment yield (SY) [5-7]. The RUSLE and SDR are empirically developed for a specific region, so their predicability is limited when applied for other regions [4, 8]. The RUSLE inputs and SDRs were proposed for biophysical conditions of Taiwan [9], that may minimize the uncertainty in soil erosion and SY predictions. Among the factors influencing soil erosion, vegetation, and land use activities are the most significant components, in addition to rainfall intensity and terrain conditions [10]. Afforestation is recognized as one of the optimal solutions for soil conservation [11]. Forest can considerably enhance water filtration, reduce runoff rate, and protect soil from erosion and runoff [12]. The cover and management (C) factor as an input of the RUSLE stands for soil protection by different land uses [13]. The C factor is determined from remote sensing and GIS data at landscape level [14]. Land use/land cover is appropriately distributed under various environmental conditions that can mitigate soil erosion intensity from human activities [15].

Fragmentation refers to the spatial transformation of landscapes, marked by habitat loss and a rise in the number of patches [16]. The process of forest fragmentation occurs due to human activities such as logging, converting forests into agricultural land, and suburban development [17]. Fragmentation adversely affects primates and other species, leading to declines in population numbers and sizes, reduced genetic diversity, and an increased risk of extinction [18, 19]. Changes in forest structure, including canopy closure and ground cover, caused by disturbances such as timber harvesting, road construction, and log skidding, can profoundly affect headwater stream ecosystems and environmental quality, both directly and indirectly [20-22]. Soil erosion following forest disturbances is increasingly becoming a concern worldwide [23]. Water erosion frequently leads to land degradation, nutrient loss, and non-point and point source pollution [24]. Thus, investigating the impact of forest disturbances on soil erosion and sediment production is crucial for effective watershed and land management strategies [25]. The composition and spatial arrangement of forest landscapes influence the delivery of various ecosystem services and should therefore be considered in forest management planning [26]. Unlike traditional forest planning, spatial forest planning focuses on the spatial arrangement of forest management activities. It takes into account factors such as the size, shape, and distribution of forest patches across the landscape [26]. However, the review revealed a scarcity of studies that integrate water provision, erosion prevention, and cultural services into spatial forest planning [26]. Recently, landscape metrics as indicators of spatial arrangement have been incorporated in soil erosion researches. Xie, et al. [27] found that PD, SHEI, and AREA_MN are key factors influencing soil conservation in the watershed off southern China. Dai, et al. [28] explored that PD and ED exhibited a positive correlation with soil conservation function, whereas AREA_MN and AI were negatively correlated with it. To date, most studies have prioritized the quantity of forest over its spatial pattern. Osewe, et al. [29] utilized morphological spatial pattern analysis using the Guidos Toolbox 3.0 to investigate forest fragmentation at Kakamega National Forest Reserve, Western Kenya during the period of 2000-2020. Chandra Pa and Kumar Gupt [30] applied the

forest fragmentation model developed by Riitters, et al. [31] to monitor the forest status in the Hazaribagh Wild Life Sanctuary. Similarly, T V, et al. [32] also used this fragmentation model to monitor forest condition from 1979 to 2013 in Uttara Kannada District, Kenya. Understanding fragmentation allows for inferences about its potential impacts which can help identify and prioritize regions and species for direct impact assessments [30, 31].

Forests play a crucial role in reducing soil erosion on sloping land. However, they have been declining due to human activities such as settlement development, agricultural expansion, and wood production, as well as natural causes like forest fires and landslides. To support effective forest planning and management, spatial information on forest cover is essential. Thus, this study aims to incorporate forest fragmentation into soil erosion modelling to analyze the relations between the fragmented classes and erosion rate. The information would be helpful for soil conservation and forest management at watershed scales.

2. Data and methodology

2.1 Study site

The ZRB, located at the central region is the largest basin in Taiwan (Fig. 1). It covers an area of $\sim 3200 \text{ km}^2$ with a main stream of $\sim 187 \text{ km}$ [33]. Among Taiwanese river basins, it generates the highest amount of sediment loads due to fragile lithology, rugged terrain, heavy rainfall, typhoons, and landslides [34]. The terrains sharply change from 0 to 3873 m within a short horizontal distance. Average annual rainfall is recorded at 2500 mm, considerably differing between the low plains (1500 mm) and mountainous regions (4000 mm). Accumulative precipitation from May to October accounts for 75% of total annual rainfall. Its upper regions are constructed of fragile materials, such as slate, shale, and sandstone [33]. With the unfavorable conditions, the ZRB is extremely prone to soil erosion on sloping land and sediment deposition at downstream.

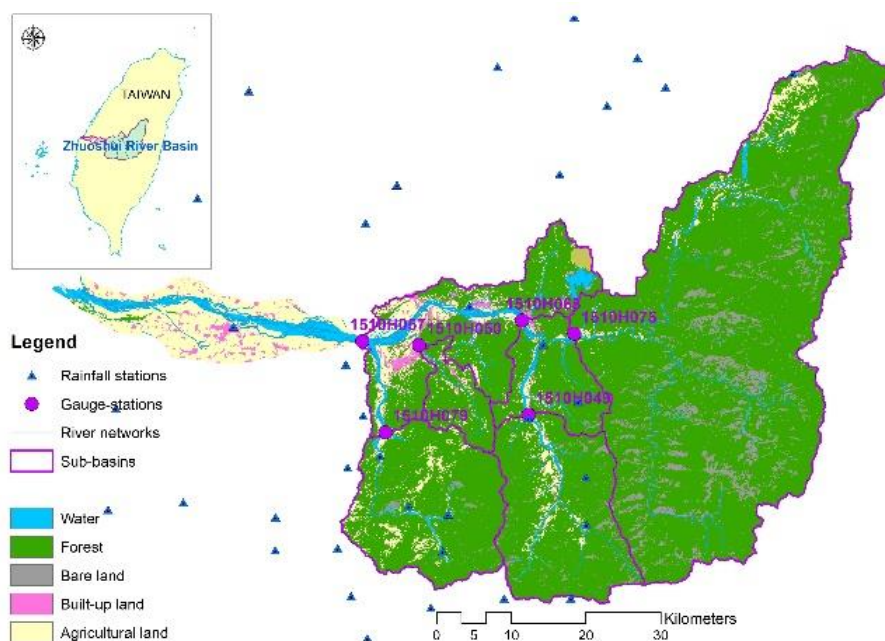


Figure 1. Location of the Zhoushui River Basin and land use/land cover in 2019.

2.2. Used data

To conduct this study, primary data from remote sensing, GIS, and station level are utilized as listed in Table 1.

Table 1. Main data acquisition.

Data	Source	Analytical purpose
Land use/Land cover	Landsat images 2019	Classify LULC types
Digital Elevation Model	United States Geological Survey (downloaded at https://earthexplorer.usgs.gov/)	Analyze topographic factors in the RUSLE
Annual rainfall	49 weather stations in and around the ZRB	Estimate rainfall erosivity factor in the RUSLE
Soil data	Taiwan Agricultural Research Institute Council of Agriculture	Estimate soil erodibility factor in the RUSLE and Slopeland capability classification
NDVI	Landsat images 2019	Estimate the vegetation cover factor in the RUSLE
Measured sediment and water discharge	Water Resource Agency of Taiwan (2005-2018)	Validate sediment yield

2.3. The RUSLE model for soil erosion prediction

The RUSLE was proposed by Wischmeier and Smith [35] and then revised by Renard et al. [36]. It is expressed as:

$$A = R \times K \times L \times S \times C \times P \quad (1)$$

where A is the average soil loss rate ($t \text{ ha}^{-1} \text{ yr}^{-1}$), R is the rainfall erosivity ($\text{MJ mm ha}^{-1} \text{ h}^{-1} \text{ yr}^{-1}$), K is the soil erodibility ($t \text{ h MJ}^{-1} \text{ mm}^{-1}$), L is the slope length, S is the slope steepness, C is the cover and management (dimensionless), and P is the conservation practice (dimensionless).

Determination of the RUSLE inputs is referred to the antecedent study for the ZRB [37, 38] as described in Table 2.

Table 2. Required inputs for the RUSLE model.

The RUSLE input	Method
Rainfall erosivity (R)	$R = 17.02 \times 0.020653 \times P^{1.35072}$; P is the annual rainfall (mm) [9]
Soil erodibility (K)	$K = (KI - 1)/200$; KI is the Taiwanese soil type index [9]
Slope and length (LS)	Algorithm by Desmet and Gover (1996) [39]
Cover and management (C)	$C = \left[\frac{1-NDVI}{2} \right]^{1+NDVI}$ [40]
Conservation practice (P)	$P = 0.2 + 0.03 \times S$; S is the slope (%) [41]

The annual rainfall data from 49 weather stations is interpolated using the co-kriging method to map its spatial distribution, which is then utilized to estimate the R factor. The LS factor is determined by the open-source SAGA software which uses the DEM as an input to produce the LS values. To derive the C factor, this study utilizes a satellite image preprocessing tool developed

by Hurni, et al. [42], which operates on Google Earth Engine. For topographic correction, the study specifically employs the physical method proposed by Dymond and Shepherd [43]. Finally, the mean C value for 2019 is computed. Regarding the P factor, it is only estimated for agriculture land, while water bodies and built-up land is set at the value of 0, and 1 for forests and bare land. Using the LULC map and slope gradient derived from the DEM, the P value for 2019 is calculated. After preparing the RUSLE inputs, these thematic layers are created at a 30-m resolution and then overlaid together to estimate the annual erosion rate, following the Eq. (1).

2.4. Sediment yield estimation using the RUSLE-SDR model

Due to a lack of soil erosion monitoring sites, the RUSLE combines with sediment delivery ratio (SDR) to estimate sediment yield (SY), which is validated with suspended sediment discharge at 6 gauge stations (as shown in Fig. 1). The SDR derived from the length and slope gradient of mainstream reveals a better SY prediction in the ZRB [37, 38].

$$SDR = 129.02 \times (L/\sqrt{S_r})^{-0.19} \quad (2)$$

where A is the watershed area in km²; L is the length of mainstream in km and S_r is the slope gradient of stream bed in percent (%). Sediment yield is determined for each sub-basin respective to its gauge station as expressed [6]:

$$SY_i = A_i \times SDR_i \quad (3)$$

where SY_i is the sediment yield for sub-basin i; A_i is the total soil erosion loss from the RUSLE for sub-basin i; and SDR_i is the sediment delivery ratio for sub-basin i. The sub-basins are presented at Fig.1, with their corresponding outlets (gauge stations). The predicted SY using the RUSLE-SDR model is checked with observed suspended sediment discharge at 6 gauge stations using the percent bias (PBIAS).

2.5. Forest fragmentation analysis

Fragmentation can accelerate the soil erosion rate, so this analysis may be helpful for forest planning in soil erosion mitigation. The forest fragmentation map is prepared from the LULC map of 2019 at a 30-m resolution using the landscape fragmentation tool from Riitters, et al. [31]. The LULC obtained from Landsat images of the year 2019 was classified by using Random forest algorithm [44]. The LULC classification results for 2019 demonstrate excellent performance, as indicated by both the high overall accuracy value and the kappa index, each reaching 0.90. The final LULC map divides the entire basin into five categories: water, forest, bare land, agricultural land, and built-up land.

The fragmentation model quantifies the extent of the forest and its presence as neighboring forest pixels within fixed-area "windows" around each forest pixel. This data is then used to categorize the window based on the type of fragmentation observed. The classification outcome is assigned to the center pixel of the window. Consequently, a pixel value on the generated map represents the fragmentation between pixels around that specific forest area. The primary analysis of the model centered on the smallest window size [31]. Grid-based fragmentation analysis after Riitters et al. (2000) is developed by a module and integrated it into SAGA software. The classification model distinguishes six types of fragmentation: (1) interior, where Pf equals 1.0; (2) patch, where Pf is less than 0.4; (3) transitional, where Pf is between 0.4

and 0.6; (4) edge, where P_f is greater than 0.6 and P_f minus P_{ff} is greater than 0; (5) perforated, where P_f is greater than 0.6 and P_f minus P_{ff} is less than 0; and (6) undetermined, where P_f is greater than 0.6 and P_f equals P_{ff} (Fig. 2). After identifying the forest fragmentation classes, a spatial analysis is conducted to obtain a mean erosion rate of each fragmentation class for 2019.

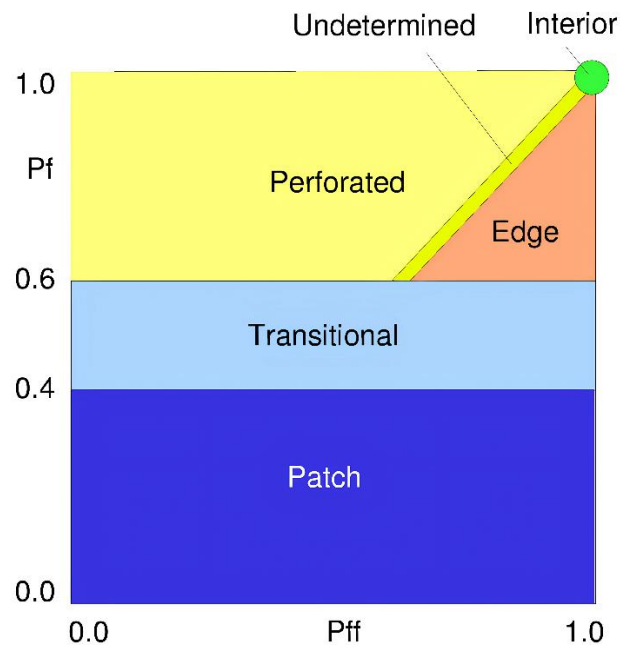


Figure 2. The model classifies forest fragmentation categories based on local measurements of P_f and P_{ff} within a fixed-area window. P_f represents the proportion of forest, while P_{ff} refers to the conditional probability that a neighboring pixel is also forested, given a forest pixel [31].

All study steps, including the performance of the RUSLE model, the RUSLE-SDR model and its validation with observed discharge recorded at gauge stations, forest fragmentation analysis, and the relationship between fragmented forest classes and soil erosion rate, are summarized in Fig. 3.

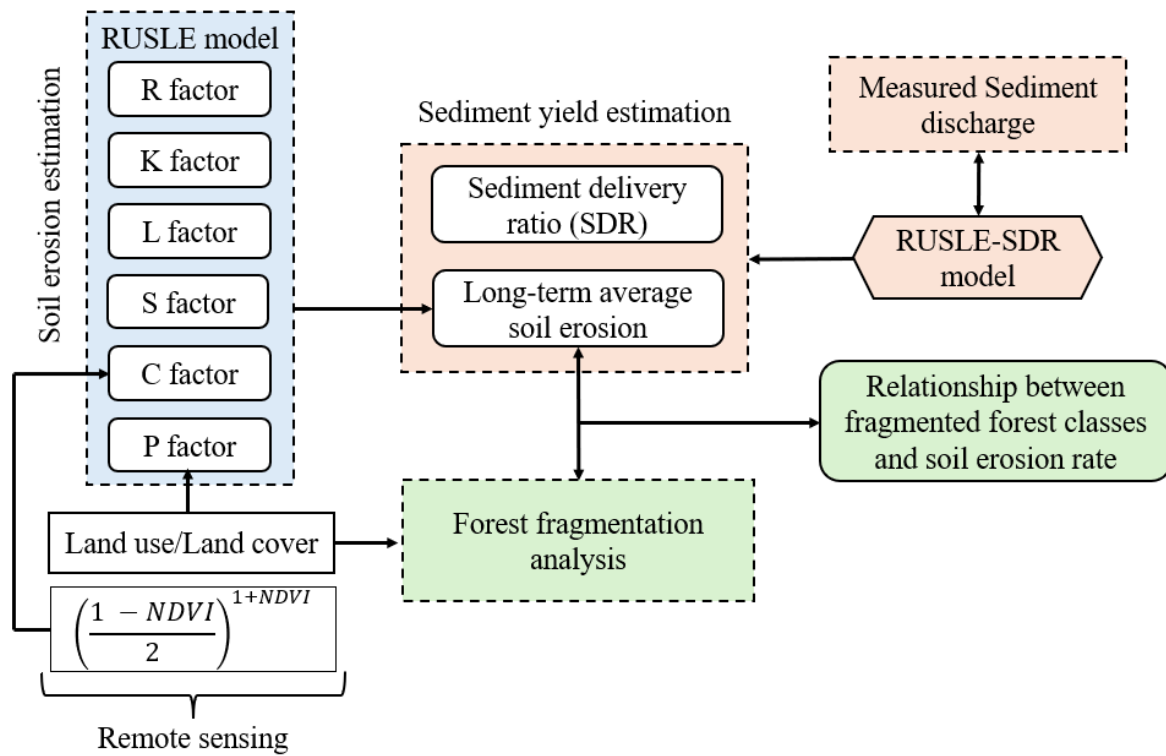


Figure 3. Overall framework of this study.

3. Results and discussions

3.1. Predicted soil erosion rate

The prediction of soil erosion rate is classified into five classes, namely mild, moderate, moderately severe, severe, and very severe (Table 3 & Fig. 4). The ZRB undergoes a severe impact from soil erosion with a mean rate of 108.47 t ha⁻¹ yr⁻¹. The moderate and moderately severe classes are dominated at 36.54% and 23.82% of the total area, respectively. The severe and very severe classes occupy nearly 21% of the total area, whereas the mild class is only 18.69% of the total area.

Table 3. Soil erosion classes for 2019.

Classes	Mild	Moderate	Moderately severe	Severe	Very severe
t ha ⁻¹ yr ⁻¹	0-10	10-50	50-100	100-150	>150
Percentage (%)	18.69	36.54	23.82	8.62	12.33

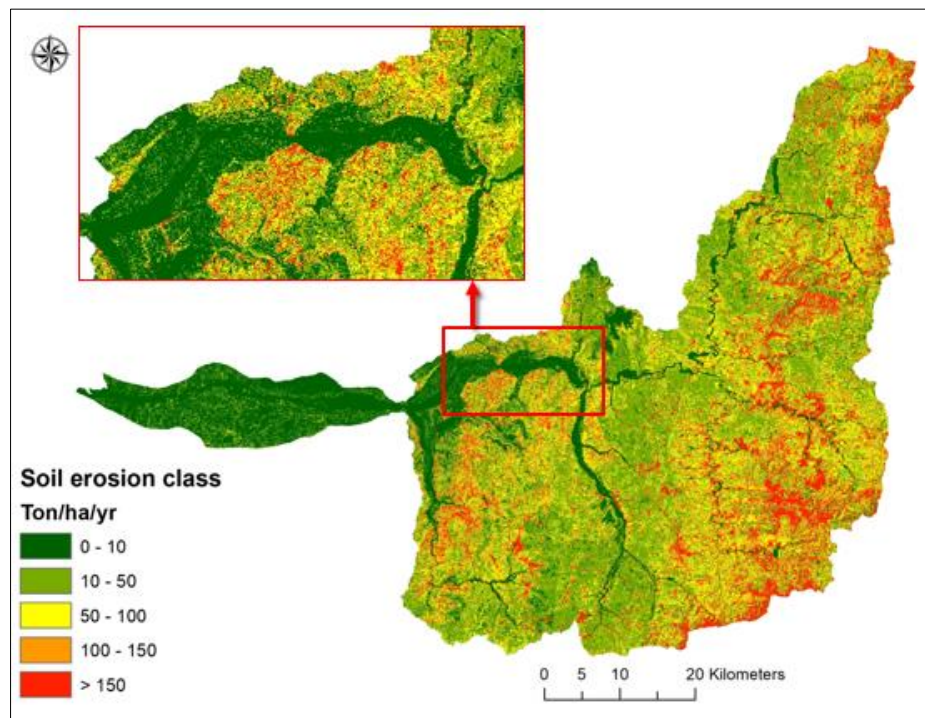


Figure 4. Soil erosion intensity classes.

Table 4 shows an annual average soil erosion rate at various LULC types. Among the five main LULC categories, bare land experiences the most severe erosion, with a mean rate of $396.58 \text{ t ha}^{-1} \text{ yr}^{-1}$. Its erosion rate significantly varies across sites, as indicated by a high standard deviation of $684.64 \text{ t ha}^{-1} \text{ yr}^{-1}$. Despite forest cover, soil resources are still subject to substantial erosion, with an estimated mean rate of $102.84 \text{ t ha}^{-1} \text{ yr}^{-1}$, with a standard deviation of $316.11 \text{ t ha}^{-1} \text{ yr}^{-1}$. On agricultural land, soil erosion rate is estimated at $22.79 \text{ t ha}^{-1} \text{ yr}^{-1}$, with a standard deviation of $72.05 \text{ t ha}^{-1} \text{ yr}^{-1}$. Several studies have assessed soil erosion in Taiwan using the RUSLE model. Using an NDVI-based approach to determine the C factor, Tsai et al. (2021) analyzed soil erosion in the Shihmen Reservoir watershed (2004-2008) reported annual erosion rates of $84.00\text{--}95.10 \text{ t ha}^{-1} \text{ yr}^{-1}$. When using a look-up table for the C factor, the erosion rate was $116.30 \text{ t ha}^{-1} \text{ yr}^{-1}$ in 2004 [45]. Chen et al. (2022) applied the USPED model to estimate a higher erosion rate of $136.40 \text{ t ha}^{-1} \text{ yr}^{-1}$ for 2004 [46]. The present study's findings align closely with these previous estimates.

Table 4. Soil erosion rate ($\text{t ha}^{-1} \text{ yr}^{-1}$) at LULC types for 2019.

LULC types	Percentage (%)	Mean	Standard deviation
Water	4.78	0.00	0.00
Forest	75.75	102.84	316.11
Bare land	6.47	396.58	684.64
Built-up land	1.90	0.00	0.00
Agricultural land	11.11	22.79	72.05

3.2. Agreement between the predicted sediment and observed sediment discharge

As mentioned in section 2.4, verifying the result of RUSLE modeling is challenging, so this study uses observed sediment discharge to compare with the predicted sediment yield from the RUSLE-SDR model. Absolute values of the PBIAS at sub-basins range from 0.75 to 24.96%, which indicates the model's performance well [47] (Table 5). It is noted that the RUSLE calculates soil

loss specifically from sheet and rill erosion, excluding other forms of erosion such as gully erosion, channel erosion, bank erosion, and mass wasting events like landslides [48]. By not accounting for these types of erosion, the RUSLE could underestimate the total amount of soil loss. Moreover, clearly, the factors influencing the SDR are highly complex, as they are linked to watershed characteristics, landforms, hydrological and climatic conditions, as well as human management practices [49].

Table 5. Summary of measured and predicted sediment (10^6 t yr^{-1}) at sub-basins

Sub-basins	Measured days	Observed sediment	SDR	A	Predicted sediment	PBIAS (%)
1510H050	328	12.00	89.33	5.90	7.41	10.88
1510H079	267	45.99	78.62	23.59	36.28	2.63
1510H049	398	32.22	81.42	32.64	42.97	0.75
1510H075	443	156.50	63.09	172.08	179.22	0.80
1510H063	401	278.46	61.37	198.36	216.59	10.17
1510H057	407	325.78	57.26	206.03	246.06	24.96

Note: Data at stations from 2005-2018, except 1510H079 (2009-2018); each sub-basin stands for its entire upper areas where water concentrates at its gauge station.

3.3. Forest fragmentation class and its corresponding soil erosion rate

Figure 5 shows a spatial distribution of forest fragmentation classes, and Table 6 presents the area, percentage, and mean erosion rate for each forest fragmentation class. The interior class occupies the largest portion of the basin, covering 50.83% of the total area, followed by the edge class at 23.33%. The perforated class accounts for only 0.68% of the total area, while the transitional and patch classes cover 5.55% and 6.60% of the total area, respectively. The spatial distribution of each fragmentation class is complicated due to both natural and anthropogenic disturbances. Generally, the patch and perforated classes are commonly observed along the river valley. These two classes are also found on the sloping areas in the upper regions, where landslides have disturbed the forested areas. The edge class is scattered throughout the basin.

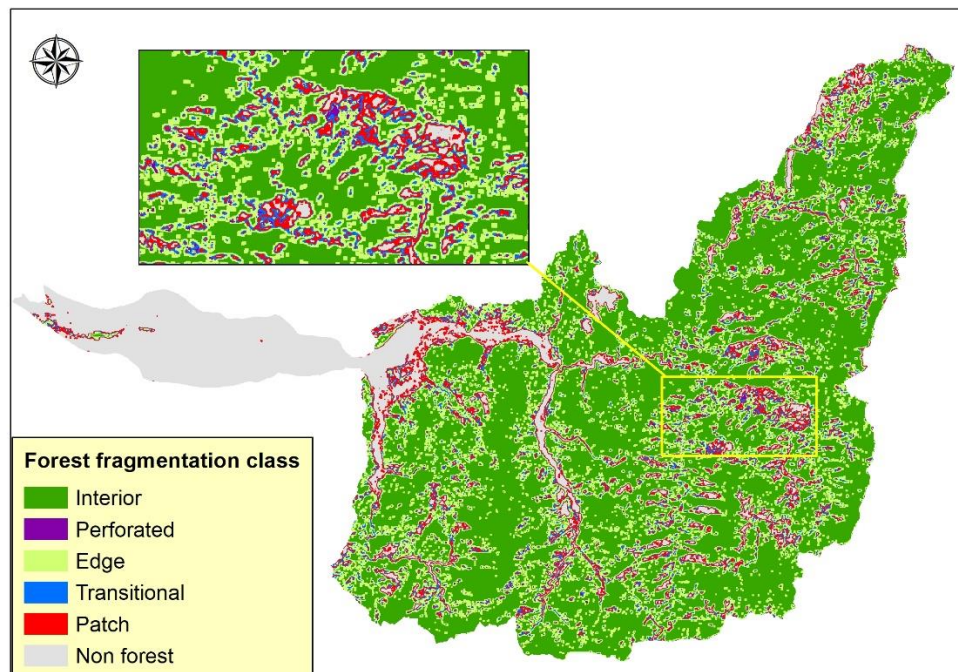


Figure 5. Forest fragmentation classes.

Soil erosion severely occurs at a mean value of over $100 \text{ t ha}^{-1} \text{ yr}^{-1}$ at forest fragmentation classes. Among them, the patch is recorded at the most detrimental impact ($266.18 \text{ t ha}^{-1} \text{ yr}^{-1}$), followed by the transitional class ($225.72 \text{ t ha}^{-1} \text{ yr}^{-1}$). The interior class receives the lowest value at $114.10 \text{ t ha}^{-1} \text{ yr}^{-1}$, and the edge and perforated classes are 136.63 and $188.76 \text{ t ha}^{-1} \text{ yr}^{-1}$, respectively.

Table 6. Soil erosion rate ($\text{t ha}^{-1} \text{ yr}^{-1}$) at forest fragmentation classes.

Fragmentation classes	Area (ha)	Percentage (%)	Mean erosion rate	Standard deviation
Interior	161092.00	50.83	114.10	379.81
Perforated	2143.26	0.68	188.76	339.58
Edge	73949.40	23.33	136.63	344.94
Transitional	17578.90	5.55	225.72	497.43
Patch	20926.50	6.60	266.18	609.66

The results indicate that interior areas are less susceptible to erosion compared to other fragmentation categories. However, these fragmented areas are more vulnerable to both natural and anthropogenic disturbances than interior regions [29]. Therefore, soil conservation activities and forest management efforts should prioritize these areas to minimize soil erosion rates.

In this study, remote sensing and fragmentation model used provide an opportunity to monitor land use or forest dynamics and their influences on ecosystem services across different scales [29, 30]. Moreover, analyzing spatial arrangement through fragmentation assessment helps forest planners develop effective strategies to enhance forest ecosystem services. However, it is noted that forest pattern analysis still depends on the spatial resolution of remote sensing images and the window size used for forest fragmentation computation.

4. Conclusions

In this study, remote sensing and GIS are utilized to assess soil erosion and forest fragmentation in the ZRB. The results show that the ZRB undergoes adverse soil erosion with a mean rate of $108.47 \text{ t ha}^{-1} \text{ yr}^{-1}$. Besides, the RUSLE-SDR model to predict SY for sub-basins is fairly checked with observed sediment data with the PBIAS values of 0.75 to 24.96%. Soil erosion is especially intense in regions suffering from forest fragmentation, with an average rate exceeding $100 \text{ t ha}^{-1} \text{ yr}^{-1}$. Among various fragmentation categories, patches exhibit the highest erosion rate at $266.18 \text{ t ha}^{-1} \text{ yr}^{-1}$. Transitional areas follow with $225.72 \text{ t ha}^{-1} \text{ yr}^{-1}$. Interior zones have the lowest erosion rate at $114.10 \text{ t ha}^{-1} \text{ yr}^{-1}$, whereas edge and perforated categories experience rates of 136.63 and $188.76 \text{ t ha}^{-1} \text{ yr}^{-1}$, respectively. Despite the basin maintaining a large proportion of its total area as forest, with 75.75% forest cover, the soil erosion rate on forest land remains high. Much more effort is needed to control soil erosion in the basin, particularly in fragmented categories with severe erosion rates. Moreover, considering the complex factors influencing soil erosion, it is essential to implement additional control measures. These measures should include engineering solutions alongside forest planting to effectively reduce soil erosion and sediment loads. This approach would be useful for monitoring forest dynamics or the effective forest planning on soil and water conservation at watershed scales.

Acknowledgments

This work was supported by Taiwan's Soil and Water Conservation Bureau under the project's codes 109 保發-11.1-保-01-06-001.

References

- [1] R. Lal, "Global overview of soil erosion," *Soil and Water Science: Key to understanding our Global environment*, vol. 41, pp. 39-51, 1994.
- [2] O. Vigiak and G. Sterk, "Empirical water erosion modelling for soil and water conservation planning at catchment-scale," *WIT Transactions on Ecology and the Environment*, vol. 46, 2001.
- [3] C. G. Karydas, P. Panagos, and I. Z. Gitas, "A classification of water erosion models according to their geospatial characteristics," *International Journal of Digital Earth*, vol. 7, no. 3, pp. 229-250, 2012.
- [4] C. Alewell, P. Borrelli, K. Meusburger, and P. Panagos, "Using the USLE: Chances, challenges and limitations of soil erosion modelling," *International Soil and Water Conservation Research*, vol. 7, no. 3, pp. 203-225, 2019.
- [5] A. Almagro *et al.*, "Improving cover and management factor (C-factor) estimation using remote sensing approaches for tropical regions," *International Soil and Water Conservation Research*, vol. 7, no. 4, pp. 325-334, 2019.
- [6] M. K. Jain and U. C. Kothyari, "Estimation of soil erosion and sediment yield using GIS," *Hydrological Sciences Journal*, vol. 45, no. 5, pp. 771-786, 2000.
- [7] J. Rajbanshi and S. Bhattacharya, "Assessment of soil erosion, sediment yield and basin specific controlling factors using RUSLE-SDR and PLSR approach in Konar river basin, India," *Journal of Hydrology*, vol. 587, 2020.

- [8] V. Ferro and M. Minacapilli, "Sediment delivery processes at basin scale," *Hydrological Sciences Journal*, vol. 40, no. 6, pp. 703-717, 1995.
- [9] SWCB, "General & Basic Investigation and Analysis," 2019, Available: https://www.swcb.gov.tw/Home/eng/Statistics/show_detail?id=4038556633c8485fb14ca42a90361194.
- [10] J. B. Thornes and J. Wainwright, *Environmental issues in the Mediterranean: processes and perspectives from the past and present*. Routledge, 2004.
- [11] V. c. H. D. Zuazo and C. R. o. R. Pleguezuelo, "Soil-erosion and runoff prevention by plant covers: a review," *Sustainable agriculture*, pp. 785-811, 2009.
- [12] M. Bredemeier, "Forest, climate and water issues in Europe. *Ecohydrology* 4: 159–167," ed, 2011.
- [13] K. Renard, D. Yoder, D. Lightle, and S. Dabney, "Universal soil loss equation and revised universal soil loss equation. Handbook of erosion modelling," *Blackwell Publ, Oxford*, pp 137167Saadat H, Adamowski J, Taye V, Namdar M, Shari F, Ale-Ebrahim S (2014) *A new approach for regional scale interrill and rill erosion intensity mapping using brightness index assessments from medium resolution satellite images*. *Catena*, vol. 113, p. 306313Shamshad, 2011.
- [14] V. Durigon, D. Carvalho, M. Antunes, P. Oliveira, and M. Fernandes, "NDVI time series for monitoring RUSLE cover management factor in a tropical watershed," *International Journal of Remote Sensing*, vol. 35, no. 2, pp. 441-453, 2014.
- [15] J. Zhou *et al.*, "Effects of precipitation and restoration vegetation on soil erosion in a semi-arid environment in the Loess Plateau, China," *Catena*, vol. 137, pp. 1-11, 2016.
- [16] J. Bogaert, R. Ceulemans, and D. Salvador-Van Eysenrode, "Decision tree algorithm for detection of spatial processes in landscape transformation," *Environmental management*, vol. 33, pp. 62-73, 2004.
- [17] R. T. Forman, *Foundations: Land Mosaics: The ecology of landscapes and regions (1995)*. Springer, 2014.
- [18] A. Estrada *et al.*, "Impending extinction crisis of the world's primates: Why primates matter," *Science advances*, vol. 3, no. 1, p. e1600946, 2017.
- [19] A. F. Palmeirim, M. Santos-Filho, and C. A. Peres, "Marked decline in forest-dependent small mammals following habitat loss and fragmentation in an Amazonian deforestation frontier," *PLoS One*, vol. 15, no. 3, p. e0230209, 2020.
- [20] F. Giadrossich *et al.*, "Modeling bio-engineering traits of *Jatropha curcas* L.," *Ecological Engineering*, vol. 89, pp. 40-48, 2016.
- [21] H. Blanco and R. Lal, *Principles of soil conservation and management*. Springer New York, 2008.
- [22] N. Hotta, T. Kayama, and M. Suzuki, "Analysis of suspended sediment yields after low impact forest harvesting," *Hydrological Processes: An International Journal*, vol. 21, no. 26, pp. 3565-3575, 2007.
- [23] F. Zheng, X. He, X. Gao, C.-e. Zhang, and K. Tang, "Effects of erosion patterns on nutrient loss following deforestation on the Loess Plateau of China," *Agriculture, ecosystems & environment*, vol. 108, no. 1, pp. 85-97, 2005.
- [24] Y. Lü, B. Fu, L. Chen, G. Liu, and W. Wei, "Nutrient transport associated with water erosion: progress and prospect," *Progress in Physical Geography*, vol. 31, no. 6, pp. 607-620, 2007.

- [25] A. Solgi, A. Najafi, and S. H. Sadeghi, "Effects of traffic frequency and skid trail slope on surface runoff and sediment yield," *International Journal of Forest Engineering*, vol. 25, no. 2, pp. 171-178, 2014.
- [26] E. Z. Baskent, J. G. Borges, and J. Kašpar, "An Updated Review of Spatial Forest Planning: Approaches, Techniques, Challenges, and Future Directions," *Current Forestry Reports*, vol. 10, no. 5, pp. 299-321, 2024.
- [27] X. Xie *et al.*, "Influence of Landscape Pattern Evolution on Soil Conservation in a Red Soil Hilly Watershed of Southern China," *Sustainability*, vol. 15, no. 2, 2023.
- [28] E. Dai, R. Lu, and J. Yin, "Identifying the effects of landscape pattern on soil conservation services on the Qinghai-Tibet Plateau," *Global Ecology and Conservation*, vol. 50, 2024.
- [29] E. O. Osewe, M. D. Niță, and I. V. Abrudan, "Assessing the Fragmentation, Canopy Loss and Spatial Distribution of Forest Cover in Kakamega National Forest Reserve, Western Kenya," *Forests*, vol. 13, no. 12, 2022.
- [30] A. Chandra Pa and S. Kumar Gupt, "Forest Canopy Density and Fragmentation Analysis for Evaluating Spatio-Temporal Status of Forest in the Hazaribagh Wild Life Sanctuary, Jharkhand (India)," *Research Journal of Environmental Sciences*, vol. 12, no. 4, pp. 198-212, 2018.
- [31] K. Riitters, J. Wickham, R. O'Neill, B. Jones, and E. Smith, "Global-scale patterns of forest fragmentation," *Conservation ecology*, vol. 4, no. 2, 2000.
- [32] R. T V, B. Setturu, and S. Chandran, "Geospatial analysis of forest fragmentation in Uttara Kannada District, India," *Forest Ecosystems*, vol. 3, no. 1, 2016.
- [33] C.-W. Kuo, C.-F. Chen, S.-C. Chen, T.-C. Yang, and C.-W. Chen, "Channel Planform Dynamics Monitoring and Channel Stability Assessment in Two Sediment-Rich Rivers in Taiwan," *Water*, vol. 9, no. 2, 2017.
- [34] L. C. Chiang, Y. C. Wang, and C. J. Liao, "Spatiotemporal Variation of Sediment Export from Multiple Taiwan Watersheds," *Int J Environ Res Public Health*, vol. 16, no. 9, May 8 2019.
- [35] W. H. Wischmeier and D. D. Smith, *Predicting rainfall-erosion losses from cropland east of the Rocky Mountains: Guide for selection of practices for soil and water conservation* (no. 282). Agricultural Research Service, US Department of Agriculture, 1965.
- [36] K. Renard, G. Foster, G. Weesies, D. McCool, and D. Yoder, "Predicting soil erosion by water: A guide to conservation planning with the Revised Universal Soil Loss Equation (RUSLE)," *Agriculture handbook*, vol. 703, pp. 25-28, 1997.
- [37] Y.-A. Liou, Q.-V. Nguyen, D.-V. Hoang, and D.-P. Tran, "Prediction of soil erosion and sediment transport in a mountainous basin of Taiwan," *Progress in Earth and Planetary Science*, 2022.
- [38] Q.-V. Nguyen, Y.-A. Liou, K.-A. Nguyen, and D.-P. Tran, "Enhancing basin sustainability: Integrated RUSLE and SLCC in land use decision-making," *Ecological Indicators*, vol. 155, p. 110993, 2023.
- [39] P. Desmet and G. Govers, "A GIS procedure for automatically calculating the USLE LS factor on topographically complex landscape units," *Journal of soil and water conservation*, vol. 51, no. 5, pp. 427-433, 1996.

- [40] W.-C. Chou, "Modelling Watershed Scale Soil Loss Prediction and Sediment Yield Estimation," *Water Resources Management*, vol. 24, no. 10, pp. 2075-2090, 2009.
- [41] C. G. Wenner, *Soil conservation in Kenya: especially in small-scale farming in high potential areas using labour intensive methods*. Soil Conservation Extension Unit, Ministry of Agriculture, 1981.
- [42] K. Hurni, A. Heinimann, and L. Würsch, "Google earth engine image pre-processing tool: background and methods," *Centre for Development and Environment, University of Bern, Switzerland*, 2017.
- [43] J. R. Dymond and J. D. Shepherd, "Correction of the topographic effect in remote sensing," *IEEE Transactions on geoscience and remote sensing*, vol. 37, no. 5, pp. 2618-2619, 1999.
- [44] L. Breiman, "Random forests," *Machine learning*, vol. 45, no. 1, pp. 5-32, 2001.
- [45] F. Tsai, J.-S. Lai, K. A. Nguyen, and W. Chen, "Determining cover management factor with remote sensing and spatial analysis for improving long-term soil loss estimation in watersheds," *ISPRS International Journal of Geo-Information*, vol. 10, no. 1, p. 19, 2021.
- [46] W. Chen, W.-H. Wang, and K. A. Nguyen, "Soil erosion and deposition in a Taiwanese watershed using USPED," *Sustainability*, vol. 14, no. 6, p. 3397, 2022.
- [47] D. N. Moriasi, J. G. Arnold, M. W. V. Liew, R. L. Bingner, R. D. Harmel, and T. L. Veith, "Model Evaluation Guidelines for Systematic Quantification of Accuracy in Watershed Simulations," *Transactions of the ASABE*, vol. 50, no. 3, pp. 885-900, 2007.
- [48] R. Benavidez, B. Jackson, D. Maxwell, and K. Norton, "A review of the (Revised) Universal Soil Loss Equation ((R)USLE): with a view to increasing its global applicability and improving soil loss estimates," *Hydrology and Earth System Sciences*, vol. 22, no. 11, pp. 6059-6086, 2018.
- [49] L. Wu, X. Liu, and X.-y. Ma, "Research progress on the watershed sediment delivery ratio," *International Journal of Environmental Studies*, vol. 75, no. 4, pp. 565-579, 2017.